STATE OF RESEARCH ON SHEAR STRENGTHENING OF RC BEAMS WITH FRCM COMPOSITES

J.H. Gonzalez-Libreros[a], C. Sabau[b], L.H. Sneed[c,1], C. Pellegrino[d], and G. Sas[e]

[a] Department of Civil, Environmental and Architectural Engineering, University of Padua, Italy jaime.gonzalez@dicea.unipd.it, +39 049-827-5585

[b] Department of Civil, Environmental and Natural Resources Engineering, Luleå University of Technology, Sweden, cristian.sabau@ltu.se +46 706-817-425

[c] Department of Civil, Architectural and Environmental Engineering, Missouri University of Science and Technology, Rolla, MO, USA, sneedlh@mst.edu, +1 573-341-4553 ([1] Corresponding author)

[d] Department of Civil, Environmental and Architectural Engineering, University of Padua, Italy, carlo.pellegrino@unipd.it, +39 049-827-5618

[e] Department of Infrastructure, Materials and Structural Engineering, NORUT, Norway, gabriel.sas@tek.norut.no +46 703-916-552

ABSTRACT

This paper summarizes the state of research on the topic of shear strengthening of RC beams using externally bonded FRCM composites. In the first part of this paper, a detailed bibliographical review of the literature on the shear strengthening of RC beams using FRCM composites is carried out, and a database of experimental tests is developed. Analysis of the database shows that FRCM composites are able to increase the shear strength of RC beams. The effectiveness of the strengthening system appears to be influenced by parameters including the wrapping configuration, matrix compressive strength relative to the concrete compressive strength, and axial rigidity of the fibers. Different failure modes have been reported, including fracture of the fibers, detachment of the FRCM jacket (with or without concrete attached), and slippage of the fibers through the mortar. A possible interaction between the internal transverse steel reinforcement and the FRCM system has also been observed. In the second part of this paper, four design models proposed to predict the contribution of the FRCM composite to the shear strength of RC beams are assessed using the database developed. Results show that the use of the properties of the FRCM composite in Models 3 and 4 instead of the fiber mechanical characteristics does not significantly increase the accuracy of the models. A simple formulation such as that proposed by Model 1, based on the bare fiber properties, is found to be more accurate for beams with or without composite detachment.

KEYWORDS

FRCM, FRP, reinforced concrete, shear, strengthening.

1. INTRODUCTION

Reinforced concrete (RC) structures are affected by external factors such as lack of maintenance, environmental conditions, or overloading that can cause deterioration and potentially diminish their structural performance. In addition, there is a growing need for upgrading existing structures in order to comply with requirements established in new design guidelines or to achieve an adequate level of performance due to the modification of expected loads caused by a change in use. The intervention of these structures requires the use of satisfactory rehabilitation and/or strengthening techniques that result in adequate behavior of the structure after the retrofitting process is carried out. Traditional techniques such as the increase of concrete section using concrete jackets or the use of externally bonded steel elements, which are common especially in developing countries, can often be considered as structurally acceptable but may not comply with modern requirements in which time- and cost-efficient interventions are usually required.

For this reason, externally-bonded fiber reinforced polymer (FRP) composites have become one of the most common intervention techniques for RC structures. Advantages of this technique include high stiffness-to-weight and strength-to-weight ratios, good fatigue characteristics, and ease of application. However, some limitations of this method, mainly related to the use of organic resins, have been pointed out [1]: (1) debonding of FRP from the concrete substrate; (2) poor behavior of epoxy resins at temperatures at or above the glass transition temperature; (3) relatively high cost of epoxy resins; (4) difficulty to apply onto wet surfaces or at low temperatures; (5) lack of vapor permeability; (6) incompatibly of epoxy resins with the substrate material; and (7) difficulty to conduct post-earthquake assessment of damage suffered by the structure. This suggests that the use of FRP might not be suitable for all applications, and new techniques that overcome some of these limitations are needed.

Composite materials that employ an inorganic cement-based matrix instead of an organic matrix allow for overcoming some of the limitations of FRP composites. Different names have been used in the literature to describe this type of composite depending on the matrix and fibers employed including textile reinforced concrete (TRC), textile reinforced mortar (TRM), fiber reinforced concrete (FRC), mineral based composites (MBC), and fiber reinforced cementitious matrix (FRCM). In this paper, the term FRCM is used to describe the aforementioned systems. FRCM composites exhibit significant heat resistance and vapor permeability and can be applied at low temperatures or onto wet surfaces [2]. The use of FRCM composites as a strengthening material for RC beams was first studied by [3-6], and their work can be considered as the starting point for the development of more recent research since their findings showed promising results. While research on the topic is still scarce, recent studies by [7-10], among others, have confirmed the effectiveness of this technique for flexural and shear strengthening and confinement of axially/eccentrically loaded RC elements.

This paper summarizes the state of research on the topic of shear strengthening of RC beams using externally bonded FRCM composites with the goal of serving as a reference point for the development of future research. In the first part of this paper, a detailed bibliographical review of the literature on the shear strengthening of RC beams using FRCM composites is carried out. This review summarizes the major findings and points out main aspects that should be addressed in future research. In the second part of this paper, design models proposed to predict the contribution of the FRCM composite to the shear strength of RC beams, including the ACI 549.4R [11] expressions, are assessed using a database of experimental results collected and compiled by the authors.

2. EXPERIMENTAL DATABASE

Fifteen articles related to shear strengthening of RC beams using FRCM composites were found in the technical literature and are summarized in Table 1. From these articles, a database that includes the characteristics and results of experimental tests of the FRCM strengthened beams was developed and is presented in Appendix A. Eighty-nine strengthened beams are included in the database.

Table 1 Summary of studies on shear strengthening of RC beams using externally bonded FRCM composites

Reference	Year	Beam Cross-sectional Shape[a]	Number of Strengthened Beams	Failure Mode		Strengthening Configuration[d]		
				Flexure[b]	Shear[c]	SB	U[(e)]	W
[9]	2006	R	3	2	1			3
[10]	2006	R	2		2			2
[12]	2008	T	9		9		9 (6)	
[13]	2009	R	7		7	7		
[1]	2012	R	8		8	8		
[14]	2013	R	6	2	4	2	4	
[15]	2014	R	6		6	3	3	
[16]	2014	R	2		2		2 (1)	
[17]	2014	T	10		10		10 (6)	
[18]	2015	R	6		6		6	
[19]	2015	R	8		8	2	6	
[20]	2015	R	7	2	5		7	
[21]	2015	R	8	1	7	3	3	2
[22]	2015	R	1		1			1
[23]	2016	R	6		6	6		1
		Total	89	7	82	31	50 (13)	8

[a]R=Rectangular, T-beam
[b]Yielding of longitudinal reinforcing steel bars followed by concrete crushing
[c]Failure mode related to FRCM debonding, fiber rupture, diagonal tension, and/or yielding of internal stirrups.
[d]SB=Side bonded, U=U-wrapped, W= Fully wrapped
[e]Numbers in parentheses indicate tests that include anchors

2.1 Evaluation of the Database and Distribution of Data

In order to evaluate the information collected in the database, the shear strength provided by the FRCM system (V_{FRCM}) is calculated by subtracting the shear strength of the corresponding control beam (V_{CON}) for each test. Although experimental specimens aimed to investigate the shear behavior of strengthened specimens are designed to attain shear failure, it is important to highlight that in some cases (seven tests, see Tables 1 and A1) the addition of the FRCM system changed the mode of failure from a brittle shear failure to a more ductile flexural failure. Specimens that failed in flexure can be considered as a lower bound of the strengthening capacity, but the behavior of beams that failed in that fashion is not further discussed in this paper.

Figures 1 to 3 present the variation of the ratio V_{FRCM}/V_{CON} as a function of the main geometrical and mechanical properties of the strengthened beams and the FRCM system. The horizontal axis of each plot is subdivided in order to evaluate the number and percentage of tests in different ranges, and values of which are labelled along the top of each graph. The points are subdivided according to the type of failure: flexural or shear. Shear failure is divided according to the presence or absence of detachment of the FRCM system from the strengthened beam. Further discussion on failure modes is presented in Section 2.2. It is important to note that the observations presented herein are based on the number and distribution of tests collected in the database and need to be validated when more test results become available

Figure 1 presents the variation of V_{FRCM}/V_{CON} as a function of the geometrical and mechanical properties of the beams (a/d=shear span to effective depth ratio; f'_c=mean cylinder compressive strength of concrete; ρ_{long}=longitudinal steel reinforcement ratio, A_s/b_wd; and ρ_w=internal transverse steel reinforcement ratio, A_w/b_ws, where A_s=longitudinal steel reinforcement area; b_w=beam width; A_w=internal transverse steel reinforcement area; and s=internal transverse steel reinforcement spacing). Figure 1 shows that the increase in shear strength attributed to the FRCM system varies from 3% to 195% with an average value of 55%. While a/d varies from 2.22 to 4.90, most specimens (65%) have values of a/d between 2.5-3.0, and 87% between 2.5-3.5, which is common for the evaluation of shear strength of RC beams. In addition, as shown by Kani [24], the transition point between beam action and arch action corresponds to a/d values ranging from 2.5 to 3.0, which also corresponds to the lowest values of shear strength in terms of average shear stress. Therefore, beams with values of a/d in this range are usually used in research to obtain a lower bound of the shear strength. For the range of a/d tested, no clear relation can be observed between V_{FRCM}/V_{CON} and a/d. 56% of the tests were performed on beams with f'_c ranging from 20-30 MPa and 78% from 20-40 MPa. These values of f'_c, which are relatively low for new structures, can be considered adequate to represent compressive strengths of many existing structures. 58% of the tests were performed on beams that had a relatively high reinforcement ratio (ρ_{long}>0.02). Although beams with such large values of ρ_{long} are not desirable in real applications, their use is explained by the experimental objective of avoiding failure by bending. Only 36% of the tests were performed on beams with transversal steel reinforcement ($\rho_w \neq$ 0.0). Unlike the previous variables, and disregarding the beams with ρ_w=0.0, a possible relationship between ρ_w and V_{FRCM}/V_{CON} can be observed. It appears that presence of a more dense distribution of stirrups (ρ_w>0.0015) reduces the effectiveness of the FRCM system. An explanation for this behavior is the possible interaction between the internal transverse steel reinforcement and the external FRCM strengthening, which has been reported for FRP composites [25-27]. A more detailed description of this phenomenon is presented in Section 2.3.

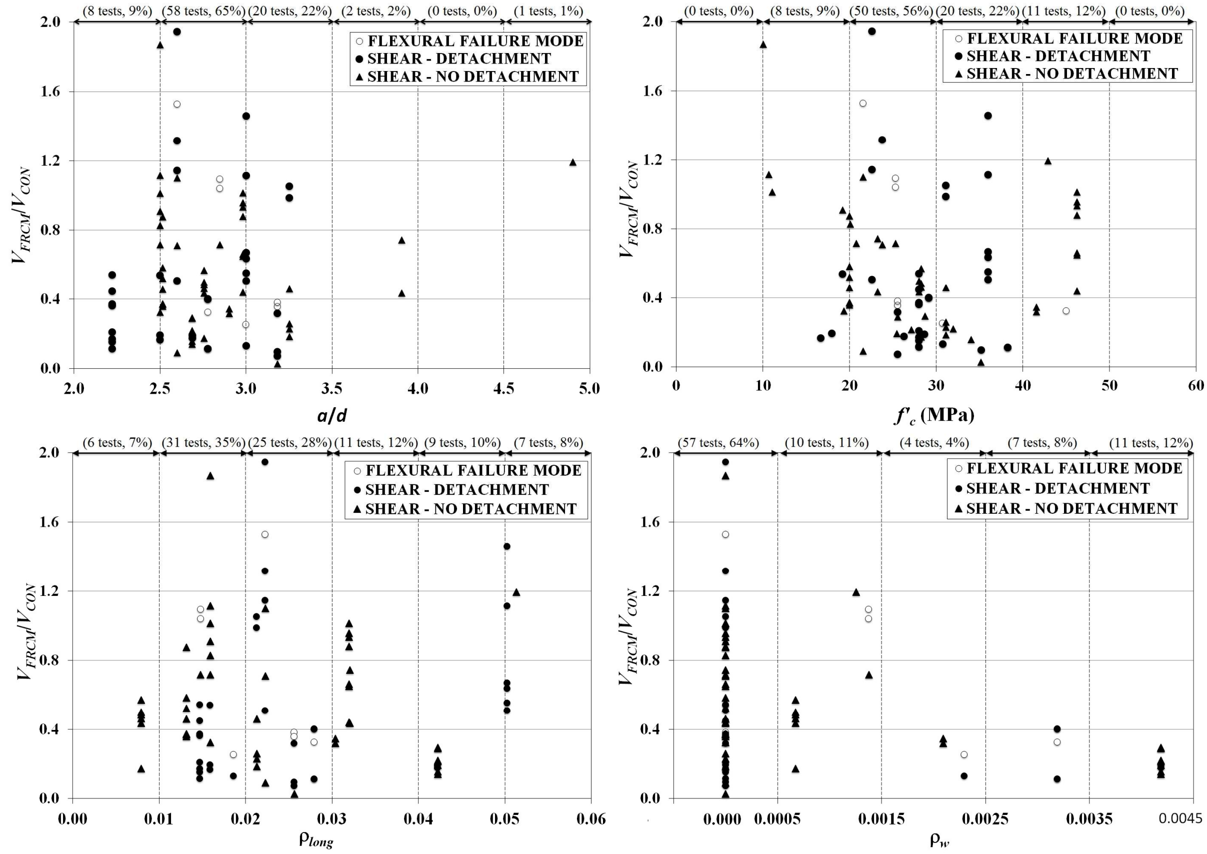

Figure 1 Variation of V_{FRCM}/V_{CON} with a/d, f'_c, ρ_{long}, and ρ_w

Figure 2 presents the variation of V_{FRCM}/V_{CON} as function of the geometrical properties of the strengthening system (strengthening configuration; n=number of fiber layers; ρ_f =fiber reinforcement ratio, $2nt_fw_f/b_ws_f$; and ρ_{cm}=FRCM reinforcement ratio, $2t_{cm}w_f/b_ws_f$, where t_f=nominal thickness of fiber sheets; w_f=width of FRCM strips; s_f=spacing of FRCM strips; and t_{cm}= total thickness of the FRCM composite $(n+1)*t_m$ with t_m the nominal thickness of a matrix layer). Most tests have been performed on beams strengthened with continuous side bonded (33%) configurations or continuous U-jackets with (26%) or without anchors (17%) configurations. Comparing the additional shear strength V_{FRCM} relative to V_{CON} for these two configurations, although slightly higher values of V_{FRCM}/V_{CON} are related to the U-continuous configuration, it is not possible to conclude that using this configuration will guarantee a better performance of the strengthened beam, which agrees with [15] who concluded that side bonded and U-wrapped configurations showed similar performance in terms of strength. In side bonded configurations detachment of the FRCM composite was less frequently observed, while for U-wrapped configuration most failures were accompanied by composite detachment, either at the composite-substrate interface or within the substrate. Although the experimental evidence is more limited, a similar behavior is also observed in beams strengthened with strips. The use of anchors with the U-wrapped configuration appears to mitigate detachment of the composite. A more detailed analysis regarding the type of failure mode and the influence of anchors is discussed in Section 2.2.

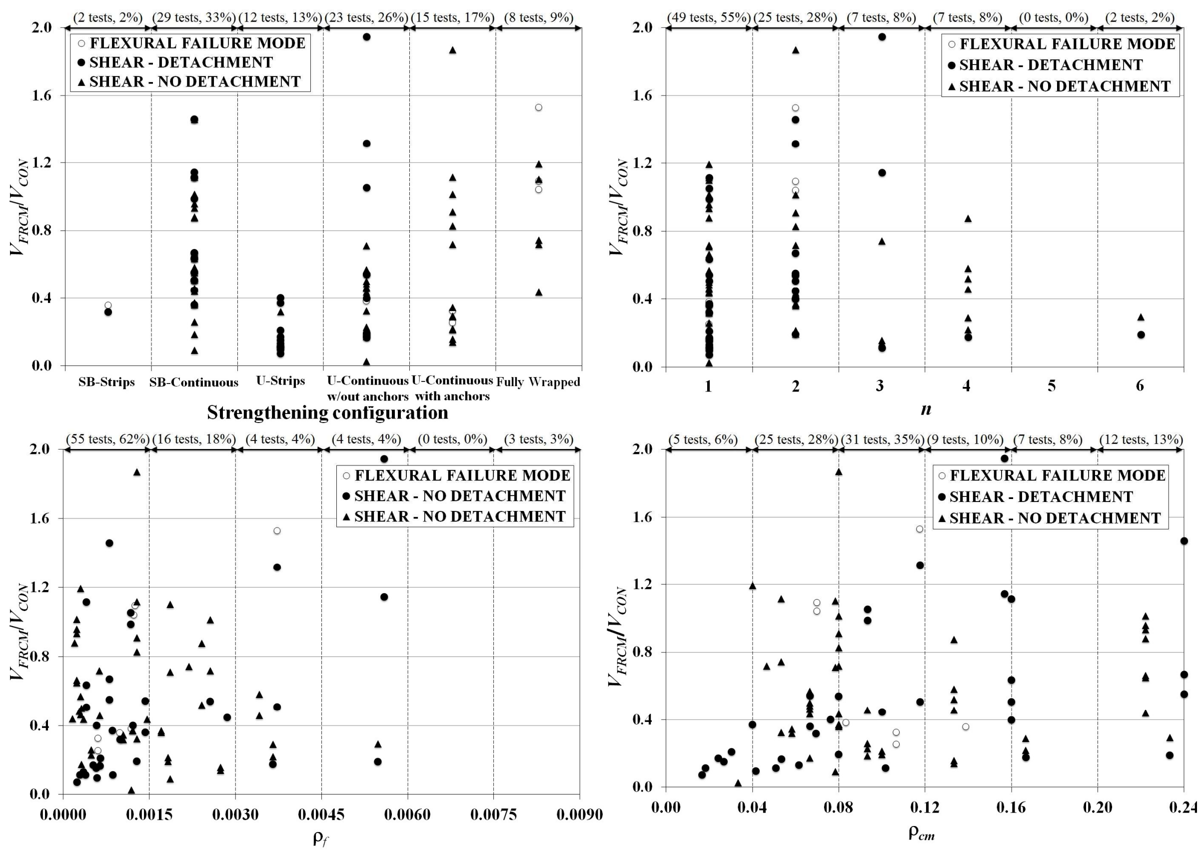

Figure 2 Variation of V_{FRCM}/V_{CON} with strengthening configuration, number of layers n, ρ_f, and ρ_{cm}

55% of the tests were carried out on beams strengthened with one layer of FRCM composite. Although some higher values of V_{FRCM}/V_{CON} can be seen increasing the number of layers from 1 to 2 or 3, the effectiveness of the system appears to be reduced when a larger number of layers are provided, i.e., the gain in shear strength may not be proportional to the number of layers. An increasing trend is observed with the increase of ρ_{cm} (that can be understood as a relative increase in the width of the concrete cross section) implying that the increase in

V_{FRCM}/V_{CON} depends not only on the amount of fibers included but also on the thickness of the cementitious matrix applied. Thicker layers of cementitious matrix, i.e. larger values of ρ_{cm}, imply a larger increase in the concrete section, and therefore an increase in the capacity of the beam would be expected, even if no fibers were included [13]. This trend is clearer for beams that failed by detachment of the composite.

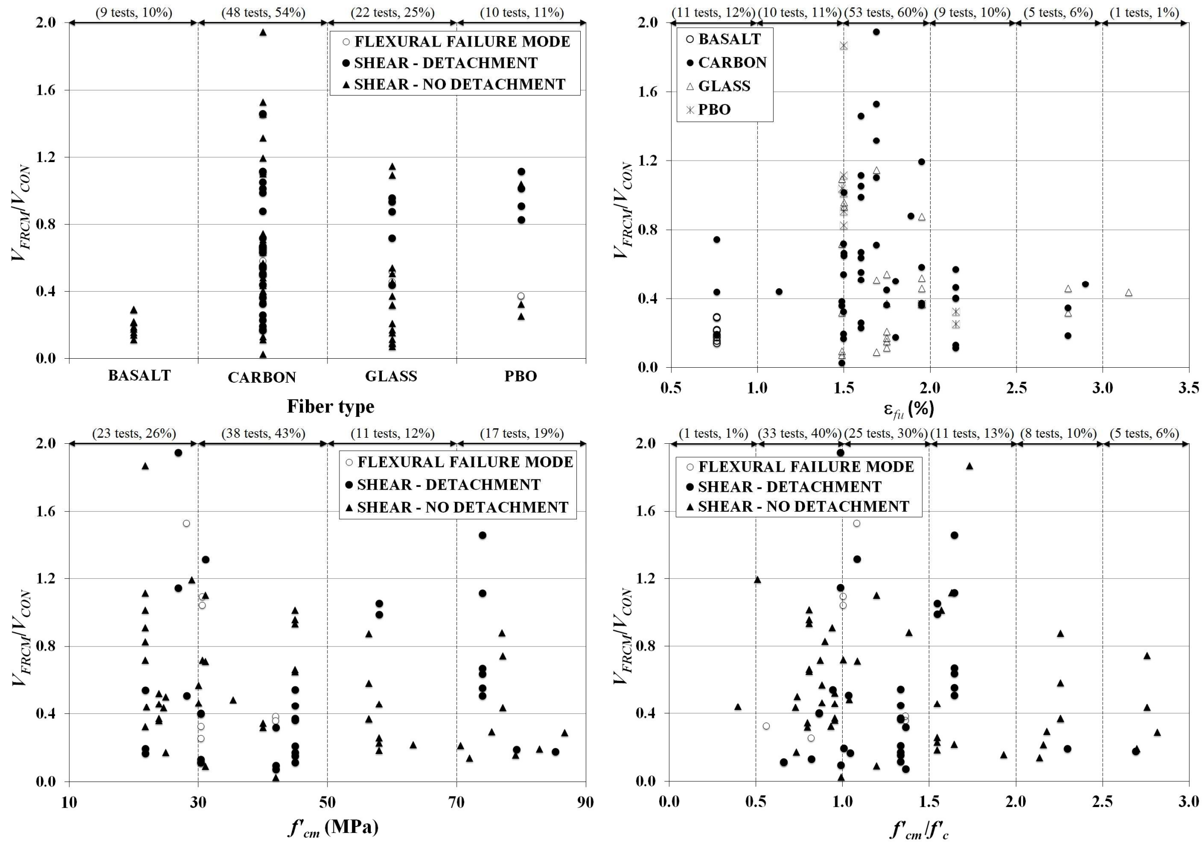

Figure 3 Variation of V_{FRCM}/V_{CON} with fiber type, fiber ultimate strain ε_{fu}, f'_{cm}, and f'_{cm}/f'_c.

In Figure 3, the influence of key mechanical properties of the FRCM composite (fiber type; bare fiber ultimate strain (ε_{fu}); cementitious matrix compressive strength (f'_{cm}); and ratio f'_{cm}/f'_c) on the ratio V_{FRCM}/V_{CON} is presented. Tests on beams with carbon fiber represent 48% of the available data, followed by glass, PBO, and basalt fibers. An important observation regarding fiber type is that beams strengthened with carbon FRCM were capable of achieving larger increases in shear strengths that beams strengthened with other type of fibers. Regarding the values of ε_{fu}, it is interesting to notice that even though there is a large dispersion for all the fibers, most tests are concentrated in a range from 1.5 to 2.0% (60% of the tests). In addition, for carbon, glass, and PBO fibers, the larger values of V_{FRCM}/V_{CON} ratios are also concentrated in the same range. Large values of f'_{cm} appear to be related to a lower effectiveness of the system (i.e., lower V_{FRCM}/V_{CON} values) . A similar trend is observed when the ratio f'_{cm}/f'_c is analyzed. It can be seen that better performance might be achieved when the compressive strengths of the substrate and the cementitious matrix are similar (f'_{cm}/f'_c close to 1.0).

2.2 Failure Modes of FRCM Strengthened Beams

Regarding fully wrapped beams, [9] reported fiber rupture and observed beam cracking clearly visible on the surface of the FRCM jacket. These findings are corroborated by [10] who reported a similar behavior. This type of failure agrees with the experimental evidence for beams fully wrapped with FRP composites, which tend to fail due to FRP rupture [27]. As noted by [28] for FRP composites, this behavior indicates that the wrapping configuration is able to provide significant anchorage to avoid composite debonding. It is worth mentioning that information on the overlap length and its design is not reported in the references but should be related to the effective length of the composite, i.e., the length needed to fully develop the load-carrying capacity of the interface [29].

It is not as straightforward to identify a typical failure mode for side bonded and U-wrap configurations as it is for fully wrapped beams. Composite detachment, which is described as debonding of the FRCM jacket from the substrate (with or without concrete attached) in this paper, is reported in some of the references [,14,19,20]. In most cases, detachment was located at the matrix-substrate surface without affecting the concrete surface, although peeling off of the concrete cover (i.e., within the substrate) has also been witnessed [21,23]. However, it is not possible to conclude that failure will be exclusively related to this phenomenon as other failure modes have also been reported in the available literature. [1,16,18] described failure caused by diagonal tension. The same behavior, together with rupture of some fibers, was observed by [13]. Azam and Soudki [15] described failure by diagonal tension associated with a large diagonal crack for most of their specimens, although the two beams that reached a higher shear strength experienced detachment and shear compression failure. Tetta *et al.* [21] reported slippage of the vertical fibers through the mortar and partial fiber rupture. According to their findings, the type of failure depends on the strengthening configuration with slippage being more pronounced in side bonded configurations and almost eliminated for fully wrapped configurations in which fiber rupture is the dominating failure mechanism. Fiber slippage is another form of debonding that has been observed in some types of FRCM composite-concrete joints [29,30,31].

Table 2 summarizes the type of failure mode reported for the different strengthening configurations for beams without anchors. It is interesting to note that the failure mode reported for most of the side bonded configurations was not related to the detachment of the FRCM composite from the substrate. This behavior does not agree with the findings for beams strengthened with FRP composites where two- or three-sided jackets fail mainly by debonding of the composite [28]. In fact, some codes for the design of externally bonded FRP composites do not allow the use of side bonded configurations for shear strengthening of RC beams [32] in order to avoid an early debonding of the system. For U-wrapped strengthened beams the prevailing failure mode is associated with detachment of the composite, although failure without detachment was reported in 35% of the tests. Considering that all unstrengthened control beams failed in shear, it is also interesting to note that the ability to transform this type of failure into a flexural failure is not exclusively limited to fully wrapped beams, although it has been rarely reported in side bonded beams.

Table 2 Failure modes of beams with different FRCM composite strengthening configurations

Strengthening Configuration	**Failure Mode**		
	Detachment	**No Detachment**	**Flexure**
Side bonded	12	18	1
U-wrapped[a]	21	13	3
Fully wrapped	0	5	3

[a]Beams with anchors are not included

2.3 Interaction Between Internal and External Shear Reinforcement

It has been noted that the interaction between internal steel reinforcement and external FRP reinforcement should be taken into account to properly predict the overall shear strength of a strengthened beam [33,34]. According to [35], the maximum contributions of steel stirrups and FRP to the shear strength are not reached simultaneously implying that their combined contribution may actually be less than the simple summation of their respective values. The possible interaction between the internal and external shear reinforcement for FRCM systems has also been reported by [13,20], who witnessed a significant reduction in the strain values measured in the stirrups of the strengthened beams when compared with the control beams at the same load levels. In fact, for the beams tested by [20], the presence of the FRCM system precluded yielding of the stirrups, as has also been reported for similar beams strengthened with FRP composites [25].

The ratio of the axial stiffness of the transverse steel reinforcement to that of the FRP composite ($\rho_w E_s/\rho_f E_f$ where E_s=elastic modulus of stirrups, and E_f=elastic modulus of the bare fibers) has been used to evaluate the internal and external shear reinforcement interaction in FRP-strengthened beams. For FRP composites the effectiveness of the strengthening system reduces when the ratio $\rho_w E_s/\rho_f E_f$ increases [25]. The same trend is observed for FRCM composites in Figure 4, in which V_{FRCM}/V_{CON} is plotted against $\rho_w E_s/\rho_f E_f$ for strengthened beams with stirrups. Results in Figure 4 suggest that, for a given amount of FRCM, increasing the amount of internal reinforcement decreases the contribution of the FRCM (i.e., lower V_{FRCM}/V_{CON} values).Having a larger internal transversal steel reinforcement ratio by providing a smaller stirrup spacing implies that more stirrups will be crossed by the critical shear crack, and they might not yield before failure of the beam. In other words, the internal shear reinforcement may not be able to achieve its design value (based on the assumption of yielding) and provide the same contribution it gives in the unstrengthened element. This implies that subtracting the control beam shear strength from the total shear strength of the strengthened beams in order to obtain V_{FRCM} may not accurately reflect the contribution of the FRCM system.

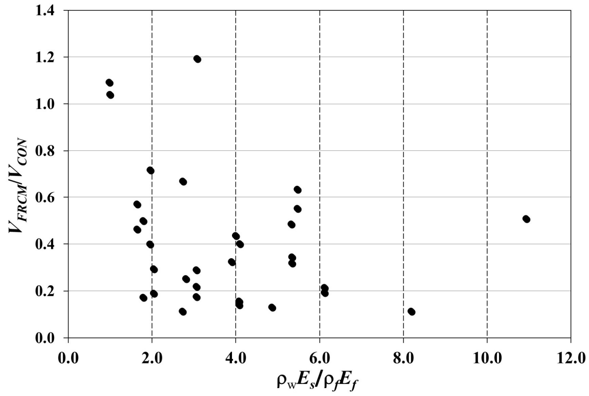

Figure 4 Variation of V_{FRCM}/V_{CON} with $\rho_w E_w/\rho_f E_f$ for strengthened beams with stirrups

2.4 Anchorage Systems

The few studies that have included anchors for the FRCM composite shear strengthening system have shown mixed results. Baggio *et al.* [16] evaluated the efficiency of FRP spike anchors for rectangular beams strengthened in shear with U-wrapped FRCM composites. The anchors, composed of carbon fibers, were inserted in predrilled holes and then fanned out. The beam with anchors showed an increase of only 3% over the strengthened beam without anchors. Although beams with and without anchors exhibited a diagonal tension shear failure, the presence of the anchors slightly changed the inclination of the shear crack around the anchors. Considering that failure of the strengthened beams by fiber slippage has been reported for certain FRCM composites [29,30,31], the lack of effectiveness of this type of anchor may be linked to the fact that they are intended to restrain out-of-plane peeling of the composite and do not restrain the in-plane fiber slippage [36].

L-shaped steel sections were used by [12] to anchor the FRCM system for U-wrapped T-beams. One leg of the steel section was glued to the FRCM composite, while the other was anchored to the bottom of the beam flange by means of vertical steel bars installed in pre-drilled holes through the entire thickness of the flange. For beams without anchors, the increase in shear capacity of the beam was approximately 19%, independent of the number of fiber layers. For beams with anchors, the shear increase strength ranged between 14% and 29%, depending on the number of layers. Although higher strengths were achieved for certain beams with anchors, the results were not consistent. However, the presence of the anchors reportedly avoided the FRCM system detachment.

Tzoura and Triantafillou [17] used a 3 mm thick curved steel section fixed to the slab with threaded rods to anchor FRCM U-wrapped T-beams. The steel sections were placed at the corners between the slab and the beam web.

The rods were placed inside 45° holes filled with an epoxy adhesive at a fixed spacing. A significant increase in the effectiveness of the FRCM jackets for the beams with anchors was reported. For beams strengthened with low textile density, the increase in strength appeared to be more significant, from approximately 18% for beams without anchors to a maximum of 187% when anchors were present. For beams with high textile density, the increase in shear strength ranged from 32% for beams without anchors to a maximum of 112% for specimens with anchors.

3. ASSESSMENT OF AVAILABLE MODELS

3.1 Overview

Four models proposed to determine the contribution of the FRCM composite to the shear strength of RC beams are evaluated in this section: Model 1 by Triantafillou and Papanicolaou [9], Model 2 by Escrig *et al.* [18], Model 3 by ACI 549.4R [11], and Model 4 by Ombres [20]. Models 1 and 2 are based on the properties of the FRCM composite fibers, and Models 3 and 4 are based on properties of the composite, as discussed in Sections 3.2 and 3.3, respectively. For the case of Model 3, which is the only guide available at this time for the design and construction of FRCM composites, the contribution to the shear strength provided by the strengthening system V_{FRCM} is considered to be additive to the strength of the unstrengthened (control) beam ($V_{CON}=V_c+V_s$), as shown in Eq. (1), in order to determine the total shear capacity of the strengthened beam V_n:

$$V_n = V_c + V_s + V_{FRCM} \tag{1}$$

where V_c and V_s are the contributions to the shear strength provided by the concrete and internal transversal steel reinforcement, respectively.

Currently there are no European standards for the evaluation of V_{FRCM}. However, it is worth noting that for the case of FRP strengthened beams, V_n in certain European-based approaches [37, 38] is computed including only V_s and the contribution of the FRP system, V_f, and its value is limited by the shear strength of the concrete compression strut, $V_{c,max}$ [39] as shown in Eq. (2).

$$V_n = min\{V_s + V_f, V_{c,max}\} \tag{2}$$

Values of V_c, V_s, and $V_{c,max}$ in Eqs. (1) and (2) are calculated using the equations in current design provisions for unstrengthened RC beams. In this paper, the evaluation of the models is carried out considering only the strength provided by the FRCM system (i.e. V_{FRCM}) and not the total shear capacity (i.e. V_n) achieved after strengthening.

Although the four models present different formulations, they are each based on the well-known truss analogy and differ mainly in the expression used to evaluate the stress (or strain) in the FRCM system along the critical shear crack. Models 1 and 3 are based on a fixed angle of the diagonal shear crack relative to the longitudinal axis (θ). Models 2 and 4 allow the use of variable angles, however only Model 2 was developed using angles different from 45° when this information was provided in the articles used to calibrate the model; otherwise the value of θ was set to 45° [18]. Therefore, and considering the limited data available reporting the actual value of θ, a fixed value of θ=45° is used in this paper to evaluate and compare the different models. It is also worth noting that in practical design applications, θ is unknown, and a fixed value of 45° is usually used.

For each model, average (AVG) values of test-to-predicted ratios of the term V_{FRCM}, denoted as V_{test}/V_{pred}, are reported, as well as the standard deviation (STD) and coefficient of variation (COV_1) computed with respect to a mean value of 1, which implies a perfect match between V_{test} and V_{pred}, as shown in Eq. (3):

$$COV_1 = \sqrt{\frac{\sum_1^N \left(\frac{V_{test,i}}{V_{pred,i}} - 1\right)^2}{N}} \tag{3}$$

where N is the number of tests. As per Section 2.1, the value V_{test} is calculated by subtracting the shear strength of the corresponding control beam (V_{CON}) for each test, whereas the value V_{pred} is computed by the model. In the assessment of the models, strengthened beams that included anchors and/or those that failed in flexure were not considered.

Different subsets of the complete database needed to be used in the assessment of the different models due to the limitations of each model and the parameters included. As mentioned earlier in this section, Models 1 and 2 use the properties of the bare fibers, and all references included in Tables 1 and A1 reported the required properties. The assessment of Model 1 is made using all tests, except those with anchors or that failed in flexure, and the resulting database is referred to as Database 1 ("DB1"), which includes 69 tests. Model 2, on the other hand, was formulated based on tests in which detachment of the FRCM system from the substrate was prevented. For this reason, its evaluation is carried out using a subset of DB1, referred to as Database 2, ("DB2"), which includes only those tests that did not exhibit composite detachment (36 tests). The performance of Models 1 and 2 is then compared using DB2 (Section 3.4), since it is common to both.

Models 3 and 4 evaluate the additional shear strength provided by the FRCM system based on the mechanical properties of the FRCM system as a composite and are presented in Section 3.3. However, only four of the references [14,18,19,20] reported the required properties of the FRCM composite. Unfortunately, the tests presented by [14] had to be disregarded because the value reported for the elastic modulus of the FRCM composite (E_{FRCM}=2.72 GPa) was approximately 50 times lower than values reported for this variable in the available literature, which resulted in values of V_{pred} that were clearly anomalous with respect to the other tests. Thus, a subset of DB1, referred to as Database 3 ("DB3") that includes 19 available tests from references that reported the mechanical properties of the composite was used to evaluate Models 3 and 4. Comparison of Models 1, 3, and 4 is carried out using DB3 (Section 3.4), since it is common to all three models. Model 2 is not included in this comparison because most tests in DB3 failed due to composite detachment of the FRCM system.

In order to facilitate the analysis, the formulations of the models are presented in this paper with a uniform notation.

3.2 Models based on properties of fibers

3.2.1 Model 1: Triantafillou and Papanicolaou [9]

Model 1 was first presented for fully wrapped rectangular beams and then extended for U-wrapped beams [17]. Assuming that the fiber is comprised of perpendicular rovings aligned perpendicular and parallel to the beam longitudinal axis, V_{FRCM} is given by Eq. (4):

$$V_{FRCM} = \rho_f \sigma_{eff} b_w d_f \tag{4}$$

where ρ_f is the geometrical reinforcement ratio of composite material, and d_f is the effective depth of the jacket taken as $0.9d$ (d=effective depth) for rectangular beams or the height of the web for T-beams. The effective stress in the FRCM system (σ_{eff}) is computed based on the average strain reached across the shear crack. Based on limited experimental evidence, [9] indicated that this strain is aproximately 50% of the ultimate strain of the bare fibers ε_{fu}, although they highlighted that further research is needed to validate this approximation. Therefore, σ_{eff} is computed by Eq. (5):

$$\sigma_{eff} = 0.5 E_f \varepsilon_{fu} \tag{5}$$

Figure 5 compares the test versus predicted values provided by the FRCM system in term of average shear stress, v_{test} and v_{pred}, where v_{test} and v_{pred} are computed according to Eqs. (6a) and (6b), respectively. The solid line v_{test}/v_{pred}=1.0 divides safe (points above the line) and unsafe (points below the line) values.

$$v_{test} = \frac{V_{test}}{b_w d} \tag{6a}$$

$$v_{pred} = \frac{V_{pred}}{b_w d} \tag{6b}$$

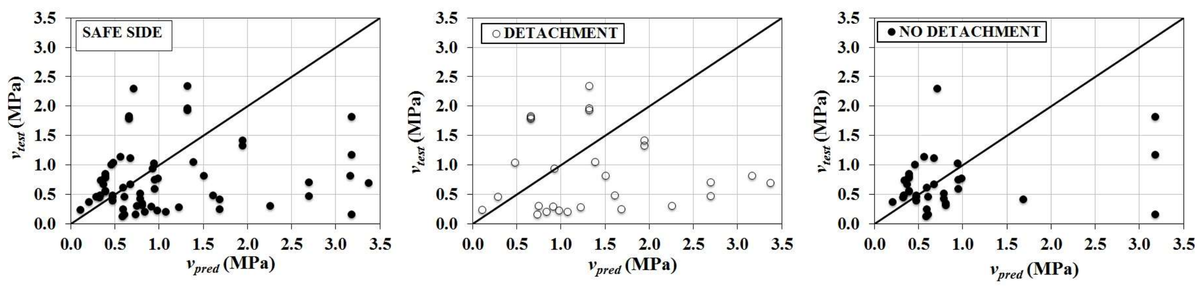

a) b) c)

Figure 5 v_{test} versus v_{pred} for Model 1: a) DB1; b) DB1-Detachment; c) DB1-No detachment

For beams that failed by detachment of the strengthening system, Figure 5b shows that Model 1 tends to overestimate (unsafe) the contribution of the FRCM composite, with AVG=0.80 (Table 3). This overestimation indicates that actual strain in the fibers might be lower than 50% of the ultimate strain assumed by the model. For beams with no detachment, the concentration of points around the solid line indicates a better agreement between predicted and test values. The AVG value for beams with no detachment is 1.12, which indicates a slight understimation (safe) of the FRCM composite contribution. Regarding the accuracy of the model, a larger value of COV_1 is associated with beams that failed by FRCM detachment.

Table 3 V_{test}/V_{pred} for Model 1 with DB1

Sample	#	AVG	STD	COV_1
Detachment	33	0.80	0.75	0.86
No Detachment	36	1.12	0.71	0.72
Total	69	0.97	0.79	0.79

Considering the limited experimental evidence used by [9] to define the value of σ_{eff}, Eq. (7) is used to determine the effective strain in the fibers ε_{eff} for the tests included in DB1. Rearranging Eq. (4), ε_{eff} can be calculated from the value of V_{test} as:

$$\varepsilon_{eff} = \frac{V_{test}}{\rho_f E_f b_w d_f} \tag{7}$$

The average value of ε_{eff} normalized by ε_{fu} (i.e., $\varepsilon_{eff}/\varepsilon_{fu}$), without including values of $\varepsilon_{eff}/\varepsilon_{fu}$>1.0, is 0.38 (COV=0.86), which is lower than the factor 0.50 proposed by the model. However, as shown in Figure 5 and Table 3, the failure mode of the beams influences the performance of the model.

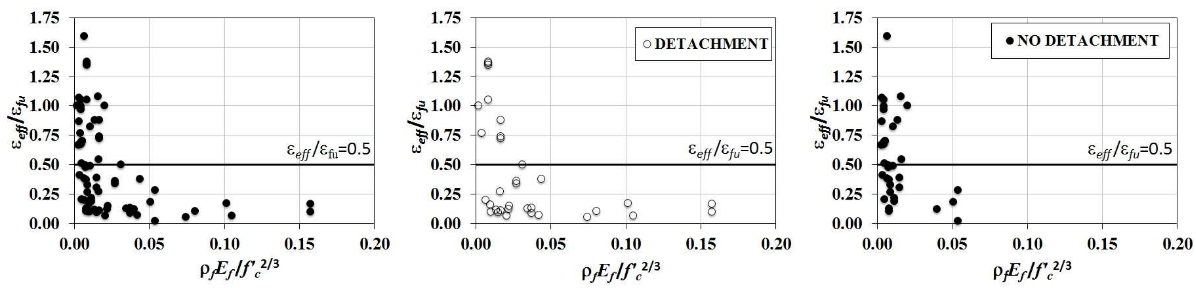

a) b) c)

Figure 6 Normalized fiber strain $\varepsilon_{eff}/\varepsilon_{fu}$ versus $\rho_f E_f/f'^{2/3}_c$: a) DB1; b) DB1-Detachment; c) DB1-No detachment

As expressed by [40] and adopted by the *fib* design model for FRP systems [37], the effective strain in the fibers depends on the axial rigidity ($E_f\rho_f$) and is inversely proportional to the tensile strength of the substrate expressed as $f'^{2/3}_c$. In Figure 6, the values of $\varepsilon_{eff}/\varepsilon_{fu}$ are plotted in terms of the ratio $\rho_f E_f/f'^{2/3}_c$, where ε_{eff} is calculated using

Eq. (7). The constant value suggested by the model ($\varepsilon_{eff}/\varepsilon_{fu}$=0.5) is also indicated in the graph. Figure 6a shows that the ratio $\varepsilon_{eff}/\varepsilon_{fu}$ tends to decrease with increasing $\rho_f E_f/f'^{2/3}_c$, as has been found for FRP composites [40]. For beams that failed by detachment (Figure 6b), ε_{eff} is generally lower than 50% of ε_{fu}, with an average of 0.28 (COV=0.85). For beams that did not show detachment, the average value is 0.46 (COV=0.58), which is close to the value proposed by the model, although the relationship of $\varepsilon_{eff}/\varepsilon_{fu}$ and $\rho_f E_f/f'^{2/3}_c$ is not as clear as for beams that failed by detachment. However, beams that did not show detachment generally present lower values of $\rho_f E_f/f'^{2/3}_c$. In fact, 80% of tests that did not fail by detachment present values of $\rho_f E_f/f'^{2/3}_c$ lower than 0.02, while only 33% of beams with detachment fall in that range. For a constant concrete strength, this finding indicates that a less stiff strengthening solution, i.e. lower values of $E_f\rho_f$, might avoid the onset of detachment. Although both detachment and shear failure can be considered as brittle failures, a better exploitation of the system can be expected with larger values of effective strain, which are associated to beams with no detachment.

3.2.2 Model 2: Escrig et al. [18]

Model 2 computes V_{FRCM} according to Eq. (8):

$$V_{FRCM} = 2n\varepsilon_{eff}E_f t_f d_f(cot\alpha + cot\theta)sin^2\alpha \tag{8}$$

where α is the fiber inclination angle with respect to the longitudinal axis of the beam, and the other variables were defined previously. Based on the research by [40] and using data collected from the literature for specimens without anchors that avoided composite detachment, [18] proposed the following equations for computing the effective strain in the fibers ε_{eff}:

- Fully wrapped:

$$\varepsilon_{eff} = 0.035\left(\frac{f'^{\,2/3}_c}{E_f\rho_f}\right)^{0.65}\varepsilon_{fu} \tag{9}$$

- Side bonded or U-wrapped:

$$\varepsilon_{eff} = 0.020\left(\frac{f'^{\,2/3}_c}{E_f\rho_f}\right)^{0.55}\varepsilon_{fu} \tag{10}$$

In Eqs. (9) and (10), E_f and f'_c are expressed in units of GPa and MPa, respectively. In Figure 7, v_{test} is plotted versus v_{pred} using Model 2 for the tests included in DB2, and Table 4 sumarizes values of AVG, STD and COV_1.

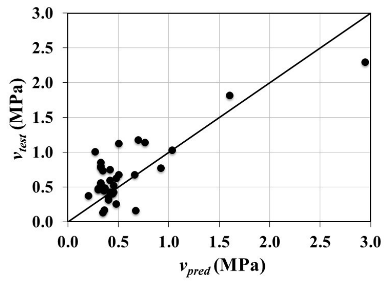

Figure 7 v_{test} versus v_{pred} for Model 2 (DB2)

Table 4 V_{test}/V_{pred} for Model 2 with DB2

Sample	#	AVG	STD	COV1
No Detachment	36	1.35	0.68	0.77

For Model 2, the effective strain in the fibers can be computed from the value of V_{test} by rearranging Eq. (8) in the form of Eq. (11):

$$\varepsilon_{eff} = \frac{V_{test}}{2nE_f t_f d_f (cot\alpha + cot\theta) sin^2\alpha} \tag{11}$$

In Figure 8, values of the ratio $\varepsilon_{eff}/\varepsilon_{fu}$ are plotted against $\rho_f E_f/f'_c{}^{2/3}$, where ε_{eff} is calculated using Eq. (11), and are shown as “calculated” in the graph. Figure 8 also includes the normalized values of ε_{eff} computed using Eqs. (9) and (10) shown as “predicted” in the graph. The relationship between $\varepsilon_{eff}/\varepsilon_{fu}$ and $\rho_f E_f/f'_c{}^{2/3}$ is not clear for beams that did not show detachment. Although a possible increase of $\varepsilon_{eff}/\varepsilon_{fu}$ with the decrease of $\rho_f E_f/f'_c{}^{2/3}$ is observed, the points do not follow the trend depicted by Eqs. (9) and (10). It is worth mentioning that for a few specimens, the value of the ratio $\varepsilon_{eff}/\varepsilon_{fu}$ is slightly larger than 1.0, implying that the effective strain is larger than the rupture strain. It should be noted that the value of ε_{eff} is not measured but rather determined by the model, and in some cases the value of the ε_{fu} is given by the manufacturer as a minimum value.

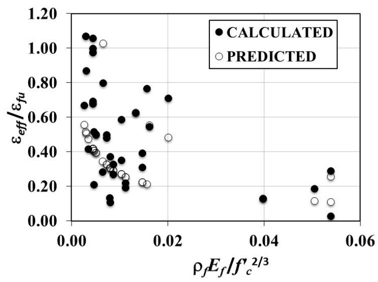

Figure 8 Normalized fiber strain $\varepsilon_{eff}/\varepsilon_{fu}$ versus $\rho_f E_f/f'_c{}^{2/3}$

3.3 Models based on properties of the FRCM composite

3.3.1 Model 3: ACI 549.4R [11]

The ACI 549.4R guideline [11] is currently the only guide for design and construction of FRCM systems. However, it is based on few experimental tests, and the guidelines note that the equations require further validation.

According to Model 3, the contribution to the shear strength of RC beams by continuous FRCM U-wrapped or continuous fully wrapped composite is computed using Eq. (12):

$$V_{FRCM} = nA_f\sigma_{eff}d \tag{12}$$

In Eq. (12), A_f is the area of mesh reinforcement per unit width effective in shear, and the other variables were defined previously. The so-called design tensile strength of the FRCM shear reinforcement σ_{eff} depends on the so-called design tensile strain of the reinforcement ε_{eff} and the tensile modulus of elasticity of the cracked FRCM composite material E_{FRCM}, and is computed using Eqs. (13) and (14):

$$\varepsilon_{eff} = \varepsilon_{FRCM,u} \leq 0.004 \tag{13}$$

$$\sigma_{eff} = E_{FRCM}\varepsilon_{eff} \tag{14}$$

Eq. (13) limits the maximum strain to the lesser of the ultimate tensile strain of FRCM composite $\varepsilon_{FRCM,u}$ and 0.004. Unfortunately, the guideline does not discuss evidence behind the 0.004 limit and/or the type of failure that is intended to be prevented by imposing this limitation. However, it is worth noting that the ACI 440.2R guide [41] imposes the same limitation for FRP composite strengthening systems to preclude the loss of aggregate interlock or delamination of FRP from the substrate for completely wrapped and two- or three-sided wrapping configurations.

Figure 9 plots v_{test} versus v_{pred} using Model 3 for the tests included in DB3, and Table 5 summarizes values of AVG, STD and COV_1. For beams that failed by detachment of the strengthening system, most points (9 of 13) fall below the v_{test}/v_{pred}=1.0 line, i.e., unsafe results, and AVG=1.03 (Table 5). For beams that did not show detachment of the FRCM composite from the substrate, all points plot above the v_{test}/v_{pred}=1.0 line with AVG= 3.70. It is important to highlight that the six tests that comprise the no detachment subgroup are from a single reference [18]. Regarding the accuracy of the model, results in Figure 9 and Table 5 show that it is highly affected by the failure mode. The COV_1 for beams with detachment is considerbly lower (0.68) than that of beams with no detachment (3.02).

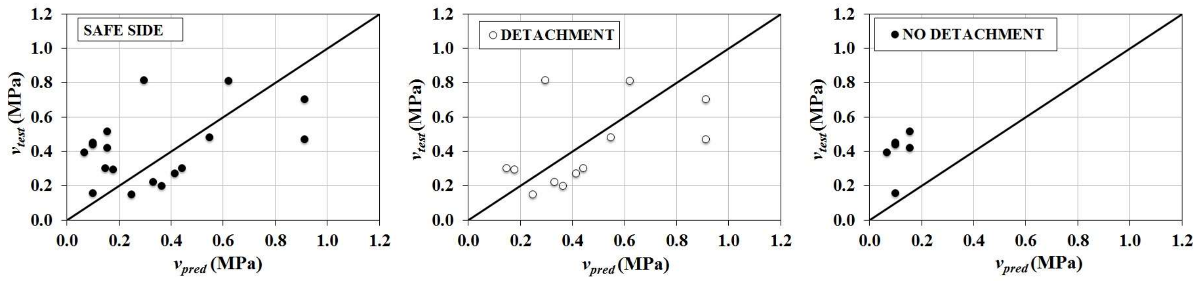

a) b) c)

Figure 9 v_{test} versus v_{pred} for Model 3: a) DB3; b) DB3-Detachment; c) DB3-No detachment

Table 5 V_{test}/V_{pred} Model 3 with DB3

Sample	#	AVG	STD	COV$_1$
Detachment	13	1.03	0.68	0.68
No Detachment	6	3.70	1.36	3.02
Total	19	1.87	1.56	1.79

A possible explanation of performance of the model could be related to the limitation of design strain imposed by the model. In fact, when Eq. (13) is applied to the 19 tests in DB3, the limiting value of 0.004 controls the value of ε_{eff} for each beam, i.e. $\varepsilon_{FRCM,u}$ is always higher than the limit imposed by the model.

Rearranging Eq. (12), Eq. (15) can be used to determine the effective strain in the FRCM composite from the value of V_{test}:

$$\varepsilon_{eff} = \frac{V_{test}}{nA_f E_{FRCM} d} \tag{15}$$

Values of $\varepsilon_{eff}/\varepsilon_{fu}$ are plotted against $\rho_f E_{FRCM}/f'_c{}^{2/3}$ for all tests in DB3 in Figure 10 where ε_{eff} is calculated using Eq. (15), and are shown as "calculated" in the graph. It is important to highlight that for this model, E_{FRCM} is used instead of E_f. Figure 10 also includes the strains used to compute V_{pred}, normalized by the ultimate strain of the FRCM composite, shown as "predicted" in the graph.

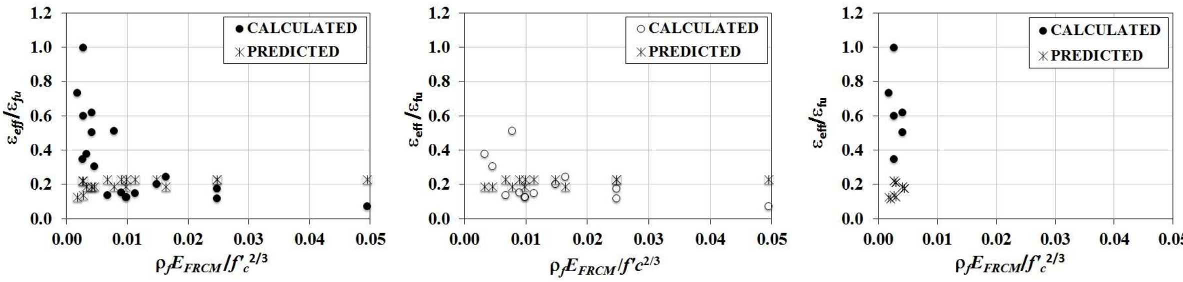

a) b) c)

Figure 10 Normalized fiber strain $\varepsilon_{eff}/\varepsilon_{fu}$ versus $\rho_f E_{FRCM}/f'_c{}^{2/3}$: a) DB3; b) DB3-Detachment; c) DB3-No detachment

Figure 10 shows that strains calculated by the model (predicted) are always lower than 25% of the ultimate strain of the composite. However, while these values appear to agree with the calculated ε_{eff} for larger values of $\rho_f E_{FRCM}/f'_c{}^{2/3}$, they do not agree for small values of $\rho_f E_{FRCM}/f'_c{}^{2/3}$. The agreement between the calculated and predicted strains is clearer for beams that failed due to detachment of the FRCM system. All beams that failed by detachment have values of $\rho_f E_{FRCM}/f'_c{}^{2/3}$ larger than 0.003, while 83% of the remaining tests (i.e., tests that showed no detachment) present lower values. This suggests that $\rho_f E_{FRCM}/f'_c{}^{2/3}$ influences the failure mode.

3.3.2 Model 4: Ombres [20]

The model by Ombres [20], developed based on the experimental response of U-wrapped beams, computes V_{FRCM}

by Eq. (16):

$$V_{FRCM} = k_e \varepsilon_{eff} E_{FRCM} \rho_f bd(cot\alpha + cot\theta)sin\alpha \tag{16}$$

where k_e is an "effectiveness coefficient" that relates the strain in an FRP system to an FRCM system and is taken as 0.5, and the other variables were defined previously.

The effective strain ε_{eff} is computed based on the formulation adopted by the 2004 Italian CNR-DT 200 Guidelines [38] shown in Eq. (17) and (18):

$$\varepsilon_{eff} = \frac{f_{fdd}}{E_{FRCM}}\left[1 - \frac{1}{3}\frac{l_e sin\alpha}{min(0.9d; h_w)}\right] \tag{17}$$

$$f_{fdd} = \frac{0.24}{\gamma_{fd}\sqrt{\gamma_c}}\sqrt{\frac{E_{FRCM} k_b \sqrt{f_{ck} f_{ctm}}}{t_f}} \tag{18}$$

where f_{ck} is the concrete characteristic strength, and f_{ctm} is the mean value of concrete tensile strength computed as:

$$f_{ctm} = 0.30 f_{ck}^{2/3} \tag{19}$$

The partial safety factors, γ_{fd} and γ_c, are set to 1.0 in this analysis. The geometric coefficient k_b is calculated with Eq. (20):

$$k_b = \left[\frac{2 - {}^{w_f}/_{b}}{1 + {}^{w_f}/_{400}}\right]^{0.5} \tag{20}$$

where b is equal to s_f for discontinuous strips or $0.9d\sin(\theta+\alpha)/\sin\alpha$ for continuous configuration. The ratio w_f/b should be larger than 0.33, otherwise the value of k_b with w_f/b equal to 0.33 shall be adopted. The optimal bond length, l_e, is defined as *"the length, if exceeded, having no increase in the force transferred between concrete and FRP"* [41]. Model 4 uses the expression in the 2004 Italian CNR-DT 200 Guidelines [38] for FRP systems to evaluate l_e and applies it to FRCM systems:

$$l_e = \left[\frac{E_{FRCM} t_f}{2 f_{ctm}}\right] \tag{21}$$

It should be noted that the term l_e has not yet been clearly defined for the case of FRCM composites. Results have shown that debonding of the FRCM-concrete interface can occur within the composite itself at the fiber-matrix interface, as opposed to the composite-concrete interface with FRP [30]. In fact, for the case of some FRCM composites where debonding is associated with slippage of the fibers relative to the embedding matrix [31], the force transferred between the concrete and the FRCM composite has been shown to increase even after the stress transfer zone (STZ) is fully established because of friction (interlocking) between fibers and the matrix in the portion of the composite where the fibers have debonded [29]. Other work suggests that the concrete strength may not significantly influence the load-carrying capatiy of the interface [42]. Therefore, the use of Eq. (21) for the case of FRCM composites may not be appropriate and requires further study.

In Figure 11, v_{test} is plotted against v_{pred} for Model 4. For beams that failed by detachment, most points fall close to the line v_{test}/v_{pred}=1.0 in Figure 11b. Figure 11c, on the other hand, shows that the model highly underestimates the contribution of the FRCM system in the overall shear strength of beams with no detachment.

Table 6 presents the values of AVG, STD, and COV_1 determined for Model 4 and the tests in DB3. For beams that failed by composite detachment, the model predicts V_{FRCM} with good accuracy with AVG=1.14 and COV_1=0.48. It is worth pointing out that five out of the 13 tests available are from [20] and therefore were used to calibrate Model 4. For beams with no detachment, the model tends to highly understimate the contribution of the FRCM system, and the accuracy is relatively low. The poorer performance of the model for beams with no detachment negatively affects the performance of the model when all 19 available tests are evaluated, as infered by the values of AVG and STD.

Table 6 V_{test}/V_{pred} for Model 4 with DB3

Sample	**#**	**AVG**	**STD**	**COV_1**
Detachment	13	1.14	0.46	0.48
No Detachment	6	2.94	0.84	2.11
Total	19	1.71	1.34	1.25

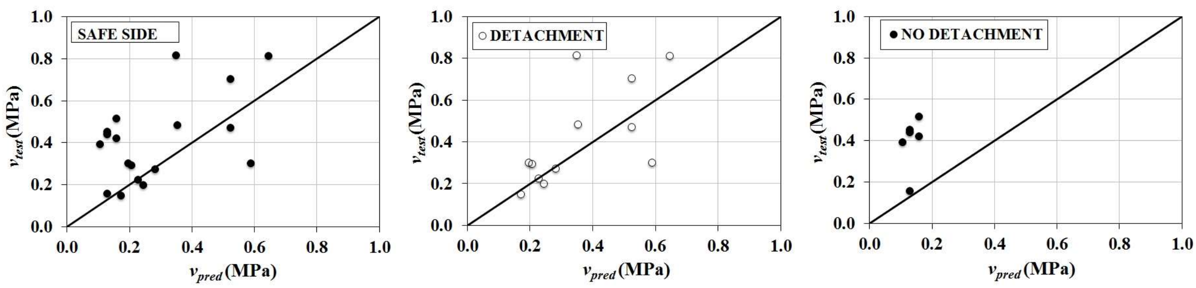

a) b) c)

Figure 11 V_{test}/V_{pred} ratios versus v for Model 4: a) DB3; b) DB3-Detachment; c) DB3-No Detachment

Rearranging Eq. (16), the effective strain can be computed from the value of V_{test} using Eq. (22):

$$\varepsilon_{eff} = \frac{V_{test}}{k_e E_{FRCM} \rho_f bd(cot\alpha + cot\theta)sin\alpha} \tag{22}$$

In Figure 12, $\varepsilon_{eff}/\varepsilon_{fu}$ ratios are plotted against $\rho_f E_{FRCM}/f'_c{}^{2/3}$, where ε_{lomg}

is calculated using Eq. (22), and are shown as "calculated" in the graph. Figure 12 also includes the normalized values of ε_{eff} computed using Eq. (17), shown as "predicted" in the graph. The behavior of Model 4 follows the same trend as Model 3 discussed in Section 3.3.1, but for beams that failed by detachment, the values of strain used by the model are always less than the 50% of the ultimate strain of the FRCM composite.

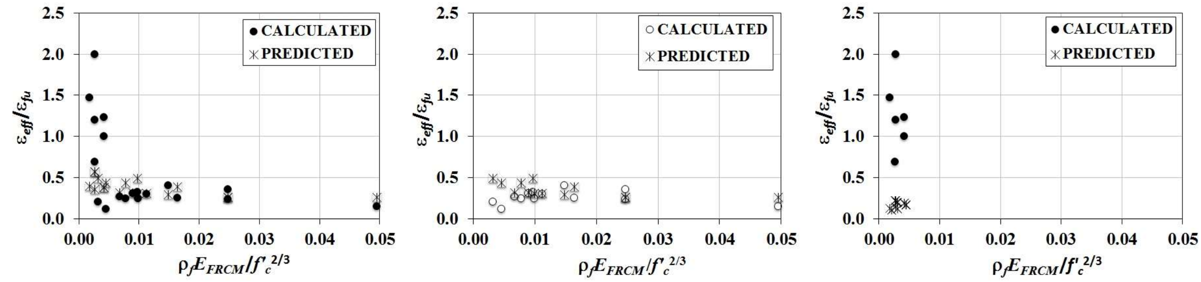

a) b) c)

Figure 12 Normalized fiber strain in terms of $\rho_f E_{FRCM}/f'_c{}^{2/3}$: a) Database 3; b) Detachment; c) No Detachment

3.4 Comparison of the performance for Models 1, 2, 3, and 4

Table 7 summarizes values of AVG, STD, and COV_1 determined for the four models studied. Since different subsets of the entire database were used in the assessment of each model, Table 7 includes the database and number of points considered for each analysis. As discussed in Section 3.1 the performance of Models 1 and 2 can be compared using DB2, since specimens in DB2 are common to both models. The performance of Models 1, 3, and 4 can be compared using DB3, since specimens in DB3 are common to all three models.

Although it was calibrated using a larger database, the AVG value obtained by Model 2 (1.35) is larger than the value obtained by Model 1 (1.12) when the common dataset DB2 is considered. The fact that Model 2 is only recommended for beams in which composite detachment is prevented limits its applicability.

Table 7 V_{test}/V_{pred} for all models with different databases

DB	Model	Failure Mode	#	AVG	STD	COV_1
1	1	Detachment	33	0.80	0.75	0.86
	1	No detachment	36	1.12	0.71	0.72
	1	All	69	0.97	0.79	0.79
2	1	Detachment	36	1.12	0.71	0.72
	2			1.35	0.68	0.77
3	1	Detachment	13	0.26	0.11	0.75
	3			1.03	0.68	0.68
	4			1.14	0.46	0.48
	1	No detachment	6	0.72	0.33	0.43
	3			3.70	1.36	3.02
	4			2.94	0.84	2.11
	1	All	19	0.40	0.30	0.67
	3			1.87	1.56	1.79
	4			1.71	1.34	1.25

The model with the AVG value closest to 1.0 is Model 3 considering only beams that failed due to detachment (1.03). On the other hand, the largest AVG is also found for Model 3 (3.70) for beams that did not show detachment. Model 1 tends to highly overestimate the contribution of the FRCM system for beams that showed detachment with AVG values as low as 0.26 (DB3). Considering tests with both failure modes, Model 3 has an

AVG of 1.87, which is somewhat misleading since its performance is highly affected by failure mode. Models based on FRCM composite properties (Models 3 and 4) have AVG values close to 1.0 for beams that showed detachment. However, these models were not capable of accurately predicting the FRCM composite shear contribution for beams that did not show detachment with large values of AVG and COV_1.

In general, although based on limited experimental evidence, Model 1 presents a more consistent behavior in terms of COV_1 for both failure modes within all the databases. However, further work is needed to validate each model presented as more data become available.

4. CONCLUSIONS

In this study, experimental results from 15 papers on shear strengthening of RC beams using externally bonded FRCM composites were collected. As result, a database that includes 89 tests was compiled, and the influence of geometrical and mechanical properties of the beams and the strengthening system was assessed. The database was also used to evaluate the performance of four models for the prediction of the contribution of the shear strength of FRCM composites to the overall strength of RC beams. The main conclusions drawn from this study are summarized as follows:

- The experimental evidence shows that FRCM composites are able to increase the shear strength of RC beams. For the beams included in the database, an increase of 3% to 195% was reported, with an average of 55%. In addition, the FRCM composite can modify the type of failure from shear to a flexural mode.
- The effectiveness of the FRCM system appears to be related to the compressive strength of the matrix, as lower values of V_{FRCM}/V_{CON} are usually found for matrixes with higher values of matrix compressive strength. The influence appears to be related to the compressive strength of the substrate, with larger values of V_{FRCM}/V_{CON} reached when the compressive strengths of the matrix and the substrate are similar.
- As for FRP composites, a possible interaction between the internal transverse steel reinforcement and the FRCM system has been observed. As reported by some researchers, the presence of the FRCM composite can limit the strain in internal stirrups and prevent them from achieving their maximum possible contribution (based on yielding), resulting in lower values of V_{FRCM}/V_{CON}. Based on the experimental tests collected in this paper, this effect appears to be more pronounced for higher values of the ratio $\rho_w E_s/\rho_f E_f$.
- For fully wrapped beams, the failure mode has been associated with fracture of the fibers. For side bonded and U-wrapped beams, detachment of the FRCM jackets (with or without concrete attached) has been reported, being the most common failure mode for U-wrapped configurations. However, failure without

detachment has also been witnessed together with diagonal cracking, slippage of the vertical fibers through the mortar, and/or partial fiber rupture.

- Although Model 1 overestimates the additional shear strength provided by the FRCM composite, it presents the more consistent behavior regarding values of COV_1 when compared with the other models. Models based on FRCM composite properties (Model 3 and 4) perform well for beams that failed by detachment, but they do not perform well for beams with no detachment.
- Although it was calibrated using a larger database, the AVG value obtained by Model 2 (1.35) is larger than the value obtained by Model 1 (1.12) considering a common dataset. In addition, the fact that Model 2 is only recommended for beams in which composite detachment is prevented limits its applicability.
- The use of the properties of the FRCM composite instead of the fiber mechanical characteristics in Models 3 and 4 does not result in a significant increase in accuracy of the models, measured in terms of COV_1. In fact, a simple formulation such as the one proposed by Model 1, based on fiber properties, is more accurate for beams with or without composite detachment.
- According to the available experimental results, strengthening solutions with values of $\rho_f E_f / f'_c{}^{2/3}$ lower than 0.02 might avoid the onset of composite detachment. It was also observed that having less stiff solutions, i.e., lower values of $\rho_f E_f$ or $\rho_f E_{FRCM}$, results in a better exploitation of the FRCM system.

The above conclusions will need to be validated when more experimental data become available. It is also hoped that the evaluation of the database and distribution of data carried out in this paper will help researchers to plan future experimental tests that focus on variables with scarce data, such as strains in internal transverse shear reinforcement, the influence of the ratio f'_{cm}/f'_c, the study of different type of fibers, and how the use of anchors help mitigate detachment and other forms of FRCM composite debonding. In addition, the inclusion of variable shear crack angles in the design models needs to be studied to evaluate their influence and potentiality improve the available models. Furthermore, the interaction between the internal and external shear reinforcement requires special attention in the development of future design models aimed to compute the final total shear capacity of a strengthened element, as the simple addition of concrete, steel, and FRCM composite contributions might not provide accurate results.

ACKNOWLEDGEMENTS

This work was supported by the European Commission (Contract number MC-ITN-2013-607851). The first and second authors would like to acknowledge the technical and economical support from the European Network for

Durable Reinforcement and Rehabilitation Solutions (*endure*), a Marie Skłodowska Curie Initial Training Network.

REFERENCES

[1] Al-Salloum, Y., Elsanadedy, M., Alsayed, S., Iqbal, R. (2012). "Experimental and numerical study for the shear strengthening of reinforced concrete beams using textile-reinforced mortar", *Journal of Composites for Constructions*, 74-90.

[2] D'Ambrisi, A., Feo, L., Focacci, F. (2013). "Experimental analysis on bond between PBO-FRCM strengthening materials and concrete", *Composites:* Part B 44: 524-532.

[3] Curbach, M., Fuchs, H., Hegger, J., Noisternig, J.F., Offermann, P., Reinhardt, H.W., Sasse, H.R., Schom, H. Woerner, J.D., Wulfhorst, B., Arnold, R., Bartl, A.-M., Bischoff, Th., Deusser, S., Doeinghaus, P. (1998). "New building material - textile concrete. A status report on current engineering developments of this new building material", *Concrete Precasting Plant and Technology* 64, 6, 45—56.

[4] Kolsch, H. (1998). "Carbon fiber cement matrix (CFCM) overlay system for masonry strengthening", *Journal of Composites for Construction 2*, 2, 105-109.

[5] Pareek, S., Kurata, M., Sotoyama, R. (2001). "Flexural strengthening of RC beams by continuous fiber sheets using polymer cement pastes as bonding agents", In *Concrete under Severe Conditions - Environement and Loading* (2324 Main Mall, Vancouver, BC, Canada V6T 1Z4, 2001), N. Banthia, K. Sakai, and O. Gjörv, Eds., University of British Columbia, Dept. of Civil Engineering, pp. 2031—2040.

[6] Kurtz, S., Balaguru, P. (2001). "Comparison of inorganic and organic matrices for strengthening of RC beams with carbon sheets", *Journal of Structural Engineering*, 127(1), 35–42.

[7] Triantafillou, T., Papanicolaou, C.G., Zissinopoulos, P., Laourdekis, T. (2006). "Concrete confinement with textile-reinforced mortar jackets", *ACI Structural Journal* 103(1): 28-37.

[8] Pellegrino, C., D'Antino, T. (2013) "Experimental behavior of existing precast prestressed reinforced concrete elements strengthened with cementitious composites", *Composite Part B: Engineering*, 55: 31–40.

[9] Triantafillou, T.C., Papanicolaou, C.G. (2006). "Shear strengthening of RC members with textile reinforced mortar (TRM) jackets", *Material Structures*, 39(1):85–93.

[10] Bruckner, A., Ortlepp, R., Curbach, M. (2006). "Textile reinforced concrete for strengthening in bending and shear", *Materials and Structures*, 39, 741-748.

[11] ACI Committee 549. (2013). "Guide to Design and Construction of Externally Bonded Fabric-Reinforced

Cementitious Matrix (FRCM) Systems for Repair and Strengthening Concrete and Masonry Structures", *ACI549.4R-13*, Farmington Hills, MI, U.S.A.

[12] Bruckner, A., Ortlepp, R., Curbach, M. (2008). "Anchoring of shear strengthening in bending and shear", *Materials and Structures*, 41, 407-418.

[13] Blanksvard, T., Taljsten, B., Carolin, A. (2009). "Shear strengthening of concrete structures with the use of mineral-based composites", *J. Compos. Constr.*, 1(25), 25–34.

[14] Contamine, R., Si Larbi, A., Hamelin, P. (2013). "Identifying the contribution of textile reinforced concrete (TRC) in the case of shear repairing damaged and reinforced concrete beams", *Engineering Structures*, 46,447–58.

[15] Azam, R., Soudki, K. (2014). "FRCM strengthening of shear-critical RC beams", *Journal of Composites for Construction.*

[16] Baggio, D., Soudki, K., Noel, M. (2014). "Strengthening of Shear Critical RC Beams with Various FRP systems", *Construction and Building Materials*. 66, 634-644.

[17] Tzoura, E., Triantafillou, T.C. (2014). "Shear strengthening of reinforced concrete T-beams under cyclic loading with TRM or FRP jackets", *Materials and Structures*.

[18] Escrig, C., Gil, L., Bernat-Maso, E., Puigvert, F. (2015). "Experimental and Analytical Study of Reinforced Concrete Beams Shear Strengthened with Different Types of Textile-Reinforced Mortar", *Construction and Building Materials*, 83, 248-260.

[19] Jung, K., Hong, K., Han, S., Park, J., Kim J. (2015). "Shear strengthening performance of hybrid FRP-FRCM", *Advances in Materials Science Engineering*, Article ID 564876.

[20] Ombres, L. (2015). "Structural performances of reinforced concrete beams strengthened in shear with a cement based fiber composite material", *Composite Structures* 122: 316-329.

[21] Tetta, Z.C., Koutas, L.N., Bournas, D.A. (2015). "Textile reinforced mortar (TRM) versus fiber-reinforced polymers (FRP) in shear strengthening of concrete beams", *Composites Part B*, 77, 338-348.

[22] Trapko. T., Urbanska. D., Kaminski, M. (2015). "Shear Strengthening of Reinforced Concrete Beams with PBO-FRCM Composites", *Composites Part B*, 80, 63-72.

[23] Awani, O., El-Maaddawy, T., El Refai, A. (2016). "Numerical Simulation and Experimental Testing of Concrete Beams Strengthened in Shear with Fabric-Reinforced Cementitious Matrix", *Journal of Composites for Construction*. DOI: 10.1061/ (ASCE)CC.1943-5614.0000711

[24] Kani G.N.J. (1967). How Safe Are Our Large Reinforced Concrete Beams?, *ACI Journal,* 128-141.

[25] Pellegrino C., Modena C. 2006. "FRP shear strengthening of RC beams: experimental study and analytical modeling", *ACI Structural Journal*, 103(5), pp. 720-728.

[26] Pellegrino C., Modena C. 2008. "An experimentally based analytical model for shear capacity of FRP strengthened reinforced concrete beams", *Mechanics of Composite Materials*, 44(3), pp. 231-244.

[27] Chen, J.F., Teng, J.G. (2003). "Shear capacity of FRP-strengthened RC beams: FRP debonding", *Composite and Building Materials*, 17, 27-41.

[28] Khalifa, A., Gold, W.J., Nanni, A., Aziz, A. (1998). "Contribution of externally bonded FRP to shear capacity of RC flexural members", *Journal of Composites for Construction*, 2(4), 195-202.

[29] D'Antino, T., Carloni, C., Sneed, L.H. Pellegrino, C. (2014). "Matrix-fiber bond behavior in PBO FRCM composites: A fracture mechanics approach", Engineering Fracture Mechanics, 117 pp. 94-111

[30] Sneed, L.H., D'Antino, T., Carloni, C. (2014). "Investigation of bond behavior of PBO fiber reinforced cementitious matrix composite-concrete interface", *ACI Materials Journal*, 111 (5) pp. 569-580.

[31] D'Antino, T., Pellegrino, C., Carloni, C., Sneed, L.H., Giacomin, G. (2015). "Experimental Analysis of the Bond Behavior of Glass, Carbon, and Steel FRCM Composites", *Key Engineering Materials*, 624, pp. 371-378.

[32] National Research Council (CNR). (2013). "Guide for the design and construction of externally bonded FRP systems for strengthening existing structures". *CNR-DT 200 R1*, Rome, Italy.

[33] Pellegrino C., Vasic, M. (2013). "Assessment of design procedures for the use of exter- nally bonded FRP composites in shear strengthening of reinforced concrete beams". Composites Part: B, 45(1).

[34] Bousselham, A., Chaallal, O. (2004). "Shear Strengthening Reinforced Concrete Beams with Fiber-Reinforced Polymer: Assessment of Influencing Parameters and Required Research", *ACI Structural Journal*, 101(2), pp. 219-227.

[35] Chen G.M., Teng J.G., Chen J.F., Rosenboom O.A. 2010. "Interaction between Steel Stirrups and Shear-Strengthening FRP Strips in RC Beams", *Journal of Composites for Construction*, 14(5), pp. 498-509.

[36] Grelle, S.V., Sneed, L.H. (2013). "Review of Anchorage Systems for Externally-Bonded FRP Laminates," *International Journal of Concrete Structures and Materials,* 7(1):17-33.

[37] Federation Internationale du Beton, *fib*. (2001). "Externally Bonded FRP Reinforcement for RC Structures", Task Group 9.3, Bulletin No. 14, Lausanne, Switzerland.

[38] National Research Council (CNR). (2004). "Guide for the design and construction of externally bonded FRP systems for strengthening existing structures". *CNR-DT 200*, Rome, Italy.

[39] D'Antino, T. & Triantafillou, T.C., 2016. Accuracy of design-oriented formulations for evaluating the

flexural and shear capacities of FRP-strengthened RC beams. *Structural Concrete,* 17(3), pp.425–442.

[40] Triantafillou, T., Antonopoulos, C. (2000). “Design of concrete flexural members strengthened in shear with FRP”. Journal of Composites for Construction, 4(4):198-205.

[41] ACI Committee 440. (2008). “Guide for the design and construction of externally bonded FRP systems for strengthening concrete structures”, *ACI 440.2R-08*, Farmington Hills, MI, U.S.A.

[42] D’Antino T., Sneed L.H., Carloni C., Pellegrino C. (2015b). “Influence of the Substrate Characteristics on the Bond Behavior of FRCM-Concrete Joints”, *Construction and Building Materials*, 101(1), pp. 838-850.

[43] Comité Européen de Normalisation (CEN): Eurocode 2: Design of concrete structures-part 1-1: general rules and rules for buildings*, EN 1992-1-1*, 2004, Brussels.

APPENDIX A

Table A1 Experimental database

			Geometry			Concrete*	Int. Reinf.		FRCM Composite												Results		
Ref.	Name	Shape	b_w [mm]	d [mm]	a/d	$f'c$ [MPa]	ρ_{long}	ρ_w	SC	Fiber	Anchors	s_f [mm]	w_f [mm]	E_f [GPa]	f_f [MPa]	n	ρ_f	f'_{cm} [MPa]	E_{FRCM} [GPa]	ρ_{cm}	Failure mode	V_{FRCM} [kN]	V_{FRCM}/V_{CON}
[9]	M2	R	150	272	2.85	25.3	0.015	0.0014	W	C	No	1	1	225	3350	2	0.0013	30.6	NR	0.070	F	63.7	1.09
	M2-s	R	150	272	2.85	25.3	0.015	0.0014	W	C	No	1	1	225	3350	2	0.0012	30.6	NR	0.070	F	60.6	1.04
	M1	R	150	272	2.85	25.3	0.015	0.0014	W	C	No	1	1	225	3350	1	0.0006	30.6	NR	0.047	S	41.8	0.72
[10]	R2	R	150	256	3.91	23.2	0.032	0.0000	W	G	No	1	1	75	574	2	0.0015	77.2	NR	0.080	S	25.5	0.44
	R3	R	150	256	3.91	23.2	0.032	0.0000	W	G	No	1	1	75	574	3	0.0022	77.2	NR	0.053	S	43.5	0.74
[12]	PB-1/1	T	120	372	2.69	25.5	0.042	0.0042	U	G	No	1	1	75	574	2	0.0018	82.8	NR	0.100	S	44.7	0.19
	PB-1/2	T	120	372	2.69	26.3	0.042	0.0042	U	G	No	1	1	75	574	4	0.0037	85.3	NR	0.167	S	41.5	0.18
	PB-1/3	T	120	372	2.69	28.6	0.042	0.0042	U	G	No	1	1	75	574	6	0.0055	79.3	NR	0.233	S	46.8	0.19
	PB-2/1	T	120	372	2.69	27.1	0.042	0.0042	U	G	Yes	1	1	75	574	2	0.0018	70.6	NR	0.100	S	51.3	0.21
	PB-2/2	T	120	372	2.69	25.6	0.042	0.0042	U	G	Yes	1	1	75	574	4	0.0037	86.7	NR	0.167	S	67.4	0.29
	PB-2/3	T	120	372	2.69	28.7	0.042	0.0042	U	G	Yes	1	1	75	574	6	0.0055	75.4	NR	0.233	S	72.4	0.29
	PB-3/1	T	120	372	2.69	28.0	0.042	0.0042	U	G	Yes	1	1	75	574	3	0.0027	72.0	NR	0.133	S	34.1	0.14
	PB-3/2	T	120	372	2.69	34.0	0.042	0.0042	U	G	Yes	1	1	75	574	3	0.0027	79.1	NR	0.133	S	42.1	0.16
	PB-3/3	T	120	372	2.69	32.0	0.042	0.0042	U	G	Yes	1	1	75	574	4	0.0037	63.3	NR	0.167	S	56.9	0.22
[13]	C40s0-M2-G2a	R	180	419	2.98	46.2	0.032	0.0000	SB	C	No	1	1	253	3800	1	0.0002	45.0	NR	0.222	S	59.9	0.96
	C40s0-M2-G2b	R	180	419	2.98	46.2	0.032	0.0000	SB	C	No	1	1	253	3800	1	0.0002	45.0	NR	0.222	S	58.4	0.93
	C40s0-M3-G2	R	180	419	2.98	46.2	0.032	0.0000	SB	C	No	1	1	201	3800	1	0.0002	77.0	NR	0.222	S	55.0	0.88
	C40s0-M2-G1	R	180	419	2.98	46.2	0.032	0.0000	SB	C	No	1	1	253	3800	1	0.0002	45.0	NR	0.222	S	41.5	0.66
	C40s0-M2-G2	R	180	419	2.98	46.2	0.032	0.0000	SB	C	No	1	1	253	3800	1	0.0002	45.0	NR	0.222	S	63.4	1.01
	C40s0-M2-G3	R	180	419	2.98	46.2	0.032	0.0000	SB	C	No	1	1	253	3800	1	0.0002	45.0	NR	0.222	S	40.7	0.65
	C40s0-M1-G3	R	180	419	2.98	46.2	0.032	0.0000	SB	C	No	1	1	262	2950	1	0.0002	22.0	NR	0.222	S	27.5	0.44
[1]	BS2	R	150	159	2.52	20.0	0.013	0.0000	SB	B	No	1	1	31.9	623	2	0.0017	23.9	NR	0.080	S	10.9	0.36
	BS3	R	150	159	2.52	20.0	0.013	0.0000	SB	B	No	1	1	31.9	623	2	0.0012	23.9	NR	0.080	S	11.3	0.37
	BS4	R	150	159	2.52	20.0	0.013	0.0000	SB	B	No	1	1	31.9	623	4	0.0034	23.9	NR	0.133	S	14.0	0.46
	BS5	R	150	159	2.52	20.0	0.013	0.0000	SB	B	No	1	1	31.9	623	4	0.0024	23.9	NR	0.133	S	15.8	0.52
	BS6	R	150	159	2.52	20.0	0.013	0.0000	SB	B	No	1	1	31.9	623	2	0.0017	56.4	NR	0.080	S	11.3	0.37
	BS7	R	150	159	2.52	20.0	0.013	0.0000	SB	B	No	1	1	31.9	623	2	0.0012	56.4	NR	0.080	S	11.3	0.37
	BS8	R	150	159	2.52	20.0	0.013	0.0000	SB	B	No	1	1	31.9	623	4	0.0034	56.4	NR	0.133	S	17.7	0.58
	BS9	R	150	159	2.52	20.0	0.013	0.0000	SB	B	No	1	1	31.9	623	4	0.0024	56.4	NR	0.133	S	26.6	0.88
[14]	R30-C-UJ-Hl-TRC(5)	R	120	204	3.18	25.6	0.026	0.0000	U	G	No	1	1	74	1102	1	0.0012	42.0	2.72	0.083	F	30.3	0.38
	R30-S-SB-P-TRC(10)	R	120	204	3.18	25.6	0.026	0.0000	SB	G	No	120	100	74	1102	1	0.0010	42.0	2.72	0.139	F	28.3	0.36
	R30-S-SB-P-TRC(5)	R	120	204	3.18	25.6	0.026	0.0000	SB	G	No	120	100	74	1102	1	0.0010	42.0	2.72	0.069	S	25.3	0.32
	R30-S-UJ-Hl-TRC(5)	R	120	204	3.18	25.6	0.026	0.0000	U	G	No	200	40	74	1102	1	0.0002	42.0	2.72	0.017	S	5.8	0.07
	R40-S-UJ-Hl-TRC(5)	R	120	204	3.18	35.2	0.026	0.0000	U	G	No	200	100	74	1102	1	0.0006	42.0	2.72	0.042	S	11.0	0.10
	R40-C-UJ-Hl-TRC(2)	R	120	204	3.18	35.2	0.026	0.0000	U	G	No	1	1	74	1102	1	0.0012	42.0	2.72	0.033	S	3.0	0.03
[15]	SB-GT	R	150	308	3.25	37.5	0.021	0.0000	SB	G	No	1	1	75	2300	1	0.0006	58.0	NR	0.093	S	11.4	0.18

			Geometry			Concrete*	Int. Reinf.		FRCM Composite													Results		
Ref.	Name	Shape	b_w [mm]	d [mm]	a/d	$f'c$ [MPa]	ρ_{long}	ρ_w	SC	Fiber	Anchors	s_f [mm]	w_f [mm]	E_f [GPa]	f_f [MPa]	n	ρ_f	f'_{cm} [MPa]	E_{FRCM} [GPa]	ρ_{cm}	Failure mode	V_{FRCM} [kN]	V_{FRCM}/V_{CON}
	UW-GT	R	150	308	3.25	37.5	0.021	0.0000	U	G	No	1	1	75	2300	1	0.0006	58.0	NR	0.093	S	28.4	0.46
	SB-CT1	R	150	308	3.25	37.5	0.021	0.0000	SB	C	No	1	1	230	3800	1	0.0005	58.0	NR	0.093	S	16.0	0.26
	UW-CT1	R	150	308	3.25	37.5	0.021	0.0000	U	C	No	1	1	230	3800	1	0.0005	58.0	NR	0.093	S	14.2	0.23
	SB-CT2	R	150	308	3.25	37.5	0.021	0.0000	SB	C	No	1	1	230	3800	1	0.0012	58.0	NR	0.093	S	61.0	0.99
	UW-CT2	R	150	308	3.25	37.5	0.021	0.0000	U	C	No	1	1	230	3800	1	0.0012	58.0	NR	0.093	S	65.0	1.05
[16]	Beam 4	R	150	310	2.90	41.6	0.030	0.0021	U	G	No	275	200	75	2300	1	0.0010	40.0	NR	0.058	S	35.5	0.32
	Beam 5	R	150	310	2.90	41.6	0.030	0.0021	U	G	Yes	275	200	75	2300	1	0.0010	40.0	NR	0.058	S	38.5	0.35
[17]	L1	T	150	320	2.50	16.7	0.016	0.0000	U	C	No	1	1	225	3375	1	0.0006	21.8	NR	0.053	S	9.6	0.17
	L2	T	150	320	2.50	18.0	0.016	0.0000	U	C	No	1	1	225	3375	2	0.0013	21.8	NR	0.080	S	11.4	0.19
	H1	T	150	320	2.50	19.4	0.016	0.0000	U	C	No	1	1	225	3375	1	0.0013	21.8	NR	0.053	S	19.9	0.32
	H2	T	150	320	2.50	19.2	0.016	0.0000	U	C	No	1	1	225	3375	2	0.0026	21.8	NR	0.080	S	33.1	0.54
	L2A15	T	150	320	2.50	20.1	0.016	0.0000	U	C	Yes	1	1	225	3375	2	0.0013	21.8	NR	0.080	S	51.8	0.83
	L2A15ha	T	150	320	2.50	19.2	0.016	0.0000	U	C	Yes	1	1	225	3375	2	0.0013	21.8	NR	0.080	S	55.6	0.91
	L2A10	T	150	320	2.50	10.1	0.016	0.0000	U	C	Yes	1	1	225	3375	2	0.0013	21.8	NR	0.080	S	84.3	1.87
	H1A15	T	150	320	2.50	10.7	0.016	0.0000	U	C	Yes	1	1	225	3375	1	0.0013	21.8	NR	0.053	S	51.9	1.12
	H2A15	T	150	320	2.50	11.1	0.016	0.0000	U	C	Yes	1	1	225	3375	2	0.0026	21.8	NR	0.080	S	48.0	1.01
	H2A10	T	150	320	2.50	20.8	0.016	0.0000	U	C	Yes	1	1	225	3375	2	0.0026	21.8	NR	0.080	S	45.6	0.72
[18]	V-BR3-01	R	300	254	2.76	28.0	0.008	0.0007	U	B	No	1	1	95	2990	1	0.0004	24.6	48	0.067	S	29.9	0.44
	V-CXM25-01	R	300	254	2.76	28.0	0.008	0.0007	U	C	No	1	1	240	4320	1	0.0003	25.0	80	0.067	S	34.3	0.50
	V-CXM25-02	R	300	254	2.76	28.3	0.008	0.0007	U	C	No	1	1	240	4320	1	0.0003	25.0	80	0.067	S	11.9	0.17
	V-PXM750-01	R	300	254	2.76	28.3	0.008	0.0007	U	PBO	No	1	1	270	5800	1	0.0003	30.0	128	0.067	S	31.9	0.46
	V-PXM750-02	R	300	254	2.76	28.3	0.008	0.0007	U	PBO	No	1	1	270	5800	1	0.0003	30.0	128	0.067	S	39.2	0.57
	V-GPHDM-02	R	300	254	2.76	28.3	0.008	0.0007	U	G	No	1	1	90	2610	1	0.0003	35.4	90	0.067	S	33.4	0.48
[19]	W600-L1	R	150	270	2.22	28.0	0.015	0.0000	SB	C	No	1	1	240	4300	1	0.0014	45.0	160	0.067	S	19.0	0.36
	W600-L2	R	150	270	2.22	28.0	0.015	0.0000	SB	C	No	1	1	240	4300	2	0.0029	45.0	160	0.100	S	23.5	0.45
	W50-N4	R	150	270	2.22	28.0	0.015	0.0000	U	C	No	183	50	240	4300	1	0.0004	45.0	160	0.018	S	6.0	0.11
	W50-N5	R	150	270	2.22	28.0	0.015	0.0000	U	C	No	138	50	240	4300	1	0.0005	45.0	160	0.024	S	9.0	0.17
	W50-N6	R	150	270	2.22	28.0	0.015	0.0000	U	C	No	110	50	240	4300	1	0.0006	45.0	160	0.030	S	11.0	0.21
	W100-N3	R	150	270	2.22	28.0	0.015	0.0000	U	C	No	250	100	240	4300	1	0.0006	45.0	160	0.027	S	8.0	0.15
	W100-N4	R	150	270	2.22	28.0	0.015	0.0000	U	C	No	167	100	240	4300	1	0.0009	45.0	160	0.040	S	19.5	0.37
	W600-N1	R	150	270	2.22	28.0	0.015	0.0000	U	C	No	1	1	240	4300	1	0.0014	45.0	160	0.067	S	28.5	0.54
[20]	TRA1	R	150	225	3.00	30.8	0.019	0.0023	U	PBO	No	1	1	270	5800	1	0.0006	30.4	128	0.107	F	19.0	0.25
	TRA2	R	150	225	3.00	30.8	0.019	0.0023	U	PBO	No	260	150	270	5800	1	0.0004	30.4	128	0.062	S	9.9	0.13
	TRB1	R	150	225	2.78	45.0	0.028	0.0032	U	PBO	No	1	1	270	5800	1	0.0006	30.4	128	0.107	F	34.2	0.32
	TRB2	R	150	225	2.78	29.2	0.028	0.0032	U	PBO	No	1	1	270	5800	2	0.0012	30.4	128	0.160	S	27.4	0.40
	TRB3	R	150	225	2.78	29.2	0.028	0.0032	U	PBO	No	210	100	270	5800	2	0.0006	30.4	128	0.076	S	27.5	0.40
	TRB4	R	150	225	2.78	38.3	0.028	0.0032	U	PBO	No	210	100	270	5800	1	0.0003	30.4	128	0.051	S	10.2	0.11
	TRB5	R	150	225	2.78	38.3	0.028	0.0032	U	PBO	No	210	100	270	5800	3	0.0009	30.4	128	0.102	S	10.2	0.11
[21]	SB_M1	R	102	177	2.60	21.6	0.022	0.0000	SB	C	No	1	1	225	3800	1	0.0019	31.1	NR	0.078	S	2.7	0.09

			Geometry			Concrete*	Int. Reinf.		FRCM Composite												Results		
Ref.	Name	Shape	b_w [mm]	d [mm]	a/d	$f'c$ [MPa]	ρ_{long}	ρ_w	SC	Fiber	Anchors	s_f [mm]	w_f [mm]	E_f [GPa]	f_f [MPa]	n	ρ_f	f'_{cm} [MPa]	E_{FRCM} [GPa]	ρ_{cm}	Failure mode	V_{FRCM} [kN]	V_{FRCM}/V_{CON}
	SB_M2	R	102	177	2.60	22.6	0.022	0.0000	SB	C	No	1	1	225	3800	2	0.0037	28.2	NR	0.118	S	15.1	0.51
	SB_M3	R	102	177	2.60	22.6	0.022	0.0000	SB	C	No	1	1	225	3800	3	0.0056	26.9	NR	0.157	S	34.0	1.14
	UW_M1	R	102	177	2.60	23.8	0.022	0.0000	U	C	No	1	1	225	3800	1	0.0019	31.1	NR	0.078	S	21.1	0.71
	UW_M2	R	102	177	2.60	23.8	0.022	0.0000	U	C	No	1	1	225	3800	2	0.0037	31.1	NR	0.118	S	39.1	1.32
	UW_M3	R	102	177	2.60	22.6	0.022	0.0000	U	C	No	1	1	225	3800	3	0.0056	26.9	NR	0.157	S	57.8	1.95
	FW_M1	R	102	177	2.60	21.6	0.022	0.0000	W	C	No	1	1	225	3800	1	0.0019	31.1	NR	0.078	S	32.7	1.10
	FW_M2	R	102	177	2.60	21.6	0.022	0.0000	W	C	No	1	1	225	3800	2	0.0037	28.2	NR	0.118	F	45.4	1.53
[22]	B1	R	150	204	4.90	42.9	0.051	0.0013	W	PBO	No	200	100	270	5270	1	0.0003	29.0	NR	0.040	S	70.1	1.19
[23]	S0-FRCM-1	R	150	250	3.00	36.0	0.050	0.0000	SB	C	No	1	1	230	3800	1	0.0004	74.0	NR	0.160	S	66.8	1.11
	S0-FRCM-2	R	150	250	3.00	36.0	0.050	0.0000	SB	C	No	1	1	230	3800	2	0.0008	74.0	NR	0.240	S	87.5	1.46
	S1-FRCM-1	R	150	250	3.00	36.0	0.050	0.0025	SB	C	No	1	1	230	3800	1	0.0004	74.0	NR	0.160	S	68.4	0.64
	S1-FRCM-2	R	150	250	3.00	36.0	0.050	0.0025	SB	C	No	1	1	230	3800	2	0.0008	74.0	NR	0.240	S	72.1	0.67
	S2-FRCM-1	R	150	250	3.00	36.0	0.050	0.0050	SB	C	No	1	1	230	3800	1	0.0004	74.0	NR	0.160	S	67.7	0.51
	S2-FRCM-2	R	150	250	3.00	36.0	0.050	0.0050	SB	C	No	1	1	230	3800	2	0.0008	74.0	NR	0.240	S	73.6	0.55

*For references reporting cube compressive strength ($f'_{c,cube}$), $f'c$ was computed according to [43]

Fiber: C=Carbon, G=Glass, B=Basalt. SC: Strengthening configuration, see Table 1. Failure mode: F=Flexure, S=Shear, see Table 1. NR=Not reported.